Ecotoxicology and Environmental Safety 280 (2024) 116544

Contents lists available at ScienceDirect

Ecotoxicology and Environmental Safety

journal homepage: www.elsevier.com/locate/ecoenv

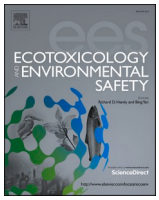

Mitigation of benzyl butyl phthalate toxicity in male germ cells with combined treatment of parthenolide, N-acetylcysteine, and 3-methyladenine

Seok-Man Kim , Gil Un Han , Seul Gi Kim , Sung-Hwan Moon , Seung Hee Shin , Buom-Yong Ryu *

Department of Animal Science and Technology, Chung-Ang University, Anseong, Gyeonggi-Do, 17546, Republic of Korea

ARTICLE INFO

Keywords:
Spermatogonia toxicity
BBP
Reactive oxygen species
Apoptosis
Autophagy
PI3K-AKT-mTOR

ABSTRACT

Benzyl butyl phthalate (BBP) is a widely used plasticizer that poses various potential health hazards. Although BBP has been extensively studied, the direct mechanism underlying its toxicity in male germ cells remains unclear. Therefore, we investigated BBP-mediated male germ cell toxicity in GC-1 spermatogonia (spg), a differentiated mouse male germ cell line. This study investigated the impact of BBP on reactive oxygen species (ROS) generation, apoptosis, and autophagy regulation, as well as potential protective measures against BBP-induced toxicity. A marked dose-dependent decrease in GC-1 spg cell proliferation was observed following treatment with BBP at 12.5 μM. Exposure to 50 μM BBP, approximating the IC_{50} of 53.9 μM, markedly increased cellular ROS generation and instigated apoptosis, as evidenced by augmented protein levels of both intrinsic and extrinsic apoptosis-related markers. An amount of 50 μM BBP induced marked upregulation of autophagy regulator proteins, p38 MAPK, and extracellular signal-regulated kinase and substantially downregulated the phosphorylation of key kinases involved in regulating cell proliferation, including phosphoinositide 3-kinase, protein kinase B, mammalian target of rapamycin (mTOR), c-Jun N-terminal kinase. The triple combination of N-acetylcysteine, parthenolide, and 3-methyladenine markedly restored cell proliferation, decreased BBP-induced apoptosis and autophagy, and restored mTOR phosphorylation. This study provides new insights into BBP-induced male germ cell toxicity and highlights the therapeutic potential of the triple inhibitors in mitigating BBP toxicity.

1. Introduction

Global urbanization has seen with it the increasing use of endocrine-disrupting chemicals (EDCs), such as phthalates and bisphenols. Consequently, environmental pollutants have gained recognition as potential contributors to male infertility in recent decades because EDC-induced hormone receptor dysfunction can affect human reproductive vitality (Dominguez, 2019; Sharma et al., 2020). Phthalate esters (PAEs) are ubiquitously utilized as plasticizers in products such as cosmetics, food packaging, toys, and various medical materials (Net et al., 2015). Because of their non-covalent binding to plastics, PAEs readily migrate to product surfaces and persist as organic pollutants that accumulate in the environment (Darbre, 2022).

Of various PAEs, benzyl butyl phthalate (BBP) exhibits slow or limited natural biodegradation (Gao and Wen, 2016). The BBP's aqueous photolysis half-life exceeds 100 days, with minimal hydrolysis of PAEs occurring under natural conditions (Gledhill et al., 1980; Staples et al., 1997). As a result, detectable levels of BBP have been found in

Abbreviations: AO, acridine orange; R/GFIR, red-to-green fluorescence intensity ratio; BBP, benzyl butyl phthalate; Spg, spermatogonia; ROS, reactive oxygen species; EDC, endocrine-disrupting chemical; PAE, phthalate ester; PI3K, phosphoinositide 3-kinase; AKT, protein kinase B; mTOR, mammalian target of rapamycin; ERK, extracellular signal-regulated kinase; JNK, c-Jun N-terminal kinase; PCNA, proliferating cell nuclear antigen; NF-κB, nuclear factor kappa B; DMEM, Dulbecco's modified Eagle's medium; FBS, fetal bovine serum; DMSO, dimethyl sulfoxide; EDTA, ethylenediaminetetraacetic acid; IC_{50}, half maximal inhibitory concentration; FACS, fluorescence-activated cell sorting; APC, allophycocyanin; DPBS, Dulbecco's phosphate buffered saline; PI, propidium iodide; RT, room temperature; PBS-T, DPBS + 0.1 % Tween 20; DCFDA, dichlorofluorescein diacetate; PBS/FBS, DPBS + 1 % FBS; DCF, dichlorofluorescein; PTL, parthenolide; 3-MA, 3-methyladenine; NAC, N-acetylcysteine; BCL2, B-cell lymphoma 2; BAX, Bcl-2-associated X protein; PARP, Poly ADP-ribose polymerase; ATG5, autophagy- related 5; ATG7, autophagy related 7.

* Corresponding author.
E-mail address: byryu@cau.ac.kr (B.-Y. Ryu).

https://doi.org/10.1016/j.ecoenv.2024.116544
Received 19 October 2023; Received in revised form 9 April 2024; Accepted 1 June 2024
Available online 4 June 2024

commercial water bottles (da Silva Costa et al., 2021), highlighting its pervasive environmental contamination in sediments, atmosphere, and soil, as a well-recognized environmental concern (Gao and Wen, 2016).

Intact spermatogenesis preserves male genetic material for subsequent generations and its disruption can lead to infertility issues (Kubota and Brinster, 2018). Although there is limited human reproductive research regarding BBP (Kavlock et al., 2002), animal studies have highlighted its detrimental effects on male reproductive health (Ahmad et al., 2014; Alam and Kurohmaru, 2016; Aso et al., 2005; Lv et al., 2019; Nagao et al., 2000). Therefore, it is crucial to investigate the specific mechanisms by which BBP impairs male reproductive function. GC-1 spermatogonia (spg), an established male germ cell line, exhibits characteristics of both Type B spermatogonia and preleptotene spermatocytes (Hofmann et al., 1992), which are pivotal stages in spermatogenesis in both humans and mice (Fayomi and Orwig, 2018), making them particularly suitable for elucidating BBP-induced toxicity at this cellular stage.

This study investigated the effect of BBP on GC-1 spg cells and examined its influence on reactive oxygen species (ROS) production, apoptosis, autophagy, and alterations in the phosphorylation levels of key signaling molecules. Furthermore, we aimed to identify potential therapeutic agents to mitigate BBP-induced male germ cell toxicity through a triple combinatorial treatment comprising ROS, nuclear factor kappa B, and autophagy inhibitors. The findings of this study not only elucidate the molecular mechanisms underlying BBP toxicity in male germ cells but also contribute to the development of potential interventions to mitigate BBP-induced toxicity.

2. Materials and methods

2.1. Chemicals, reagents, and equipment

Detailed information on chemicals, reagents, antibodies, and equipment is provided in Tables S1–S2.

2.2. GC-1 spg cell culture and BBP treatment

GC-1 spg cells (CRL-2053, ATCC, Manassas, VA, USA) were cultured in Dulbecco's modified Eagle's medium (DMEM) supplemented with 10% fetal bovine serum (FBS) and 1% penicillin/streptomycin at 37°C with 5% CO_2 in a humidified incubator. For BBP treatment, phenol red-free DMEM supplemented with 1% FBS and 1% penicillin/streptomycin (defined as the basal medium in this study) was used to minimize the effects of the growth factors and hormones contained in FBS.

BBP was dissolved in dimethyl sulfoxide (DMSO) to a final concentration of 1 M. Further serial dilutions were prepared to obtain treatment stocks of 6.25, 12.5, 25, 50, and 100 mM, along with vehicle control (0.1% DMSO in basal medium, which exhibited no toxicity, as shown in Fig. S1), to achieve final BBP concentrations of 0, 6.25, 12.5, 25, 50, and 100 μM. To treat cells with BBP, GC-1 spg cells were seeded at a density of 7×10^4 cells/well in a six-well plate for 24 h. After 24 h, BBP-containing basal medium was added and GC-1 spg cells were cultured for another 48 h for the proliferation assay.

2.3. BBP cytotoxicity assessment

To evaluate the toxic effects of BBP on GC-1 spg cells, the cells were seeded at a density of 7×10^4 cells/well in a six-well culture plate. Subsequently, the cells were treated with BBP at the concentrations as described in Section 2.2. After BBP treatment for 48 h, cells were collected using 0.25 % trypsin-ethylenediaminetetraacetic acid (EDTA) and centrifugated for 6 min at 600 × *g* at 4°C. The cells were then resuspended in a basal medium. An equal volume (10–20 μL) of GC-1 spg cell suspension was mixed with 10–20 μL of trypan blue solution for cell counting. The cell counts were determined using a hemocytometer under a microscope. The cell proliferation rate was calculated using the following equation:

$$\text{Proliferation rate}(\%) = \frac{\text{Number of harvested BBP-treated cells}}{\text{Number of seeded cells}} \times 100$$

$$\text{Relative proliferation rate}(\%) = \frac{\text{Proliferation rate of BBP-treated cells}}{\text{Proliferation rate of control cells}} \times 100$$

The half-maximal inhibitory concentration (IC_{50}) was determined as previously described (Toma et al., 2017).

2.4. Apoptosis analysis using annexin V staining

To measure BBP-induced apoptosis in GC-1 spg cells, an annexin V conjugated with allophycocyanin (APC) apoptosis kit was used to verify the apoptosis rate. Briefly, the GC-1 spg cells treated with BBP were collected using 0.25 % trypsin-EDTA and centrifugation was performed for 6 min at 600 × *g* at 4°C. Cells collected from each group were counted and washed once with Dulbecco's phosphate-buffered saline (DPBS). Subsequently, GC-1 spg cells from the control and BBP groups were resuspended in 1× binding buffer at a concentration of 1.0×10^6 cells/mL. Each group's cell suspension was aliquoted into 100 μL portions (1.0×10^5 cells) and incubated with annexin V-APC and propidium iodide (PI) for 15 min at room temperature (RT, 23–25°C in this study) in the dark. Before fluorescence-activated cell sorting (FACS) analysis, 400 μL of 1× binding buffer was added to each treatment. Annexin V assay was performed using an FACS Aria II cell sorter (Table S1).

2.5. Western blot analysis

Total cellular proteins were isolated using Totex lysis buffer (Shin et al., 2014), with occasional vortexing every 5 min for 30 min on ice. The lysate was centrifugated at 17,950 × *g* at 4°C for 30 min. The soluble proteins were transferred to new tubes and quantified using the Bradford assay. Equal amounts (10–20 μg) of each protein sample were loaded onto 6–15 % Tris-glycine sodium dodecyl sulfate polyacrylamide gels. Separated proteins were transferred onto polyvinylidene difluoride membranes activated with methanol. Following the blocking of nonspecific binding using 5 % skimmed milk dissolved in DPBS and 0.1 % Tween 20 (PBS-T) for 1 h at RT, the membranes were washed briefly with PBS-T before incubation with primary antibody overnight at 4°C with gentle shaking. Secondary antibody binding was performed in PBS-T containing 1 % bovine serum albumin and incubated for 2 h at RT. The membrane was washed thrice with PBS-T. Protein expression was visualized using two electrochemiluminescent pico- or WestGlow™ femto-ECL systems. The images of the detected proteins were acquired using a Touch Imager (Table S1). Detailed antibody information is provided in the Table S2. Band intensity was assessed using ImageJ software (version 1.8.0; National Institutes of Health, Bethesda, MD, USA) for comparisons between treatments. Intensity data were normalized to that of the loading control (α-tubulin) in all independent experiments (n = 3).

2.6. Dichlorofluorescein diacetate (DCFDA) fluorescence microscopy

To verify whether BBP induces ROS production, 2′,7′- DCFDA staining was performed (Yu et al., 2021). Briefly, GC-1 spg cells were seeded in a six-well plate at a concentration of 7×10^4 cells/well and cultured for 24 h. Subsequently, cells were treated with either DMSO control or BBP and incubated for 48 h, followed by washing with PBS/FBS (DPBS + 1% FBS) before incubation at 37°C for 45 min with 10 μM DCFDA diluted in a basal medium. Following incubation, DCFDA-diffused cells were washed twice with PBS/FBS and stained with 4 μg/mL Hoechst 33342 at 37°C for 10 min to visualize the nuclei. After a single wash with cold PBS/FBS, fluorescent images were captured using a fluorescence microscope connected to NIS Elements imaging software (Table S1, Version 5.11.00). The percentage of dichlorofluorescein (DCF)-positive GC-1 spg cells was calculated (n = 3).

2.7. Autophagy assay using acridine orange (AO) staining

AO staining was used to visualize the BBP-induced autophagic activity. As described previously, GC-1 spg cells were seeded and treated in a confocal dish for 48 h. Subsequently, the cells were rinsed once with PBS/FBS and incubated with 1 μg/mL of AO at 37°C for 15 min. Following incubation, the AO-labeled cells were washed twice with PBS/FBS and counterstained with Hoechst 33342 dyes for 10 mins at 37°C. After a single wash with chilled PBS/FBS, AO (red and green fluorescence) and Hoechst 33342 fluorescence images were captured using the confocal microscope (Table S1). The red-to-green intensity ratio (R/GFIR) was calculated as:

R/GFIR = Intensity of red fluorescence per cell / Intensity of green fluorescence per cell.

Relative value of R/GFIR (fold change) = R/GFIR of BBP-treated cells / R/GFIR of control cells.

2.8. Mitigation approach with inhibitors

To assess the alleviation efficacy of BBP-induced toxicity, three inhibitors were examined under single, dual, and triple combination conditions: N-acetylcysteine (NAC, 1 mM in basal medium), parthenolide (PTL, 1 μM in DMSO), 3-methyladenine (3-MA, 0.1 μM in DMSO). The effects of single, dual, and triple inhibitors were examined using a DMSO control and 50 μM BBP, with or without inhibitor treatments. Briefly, 7×10^4 GC-1 spg cells were cultured in a six-well plate either with DMSO as a control or inhibitor(s) for 24 h. Following this, the medium was removed, and fresh medium containing DMSO (vehicle control), BBP (hazard control), or BBP and inhibitor(s) (evaluation test conditions) was added and incubated for 48 h. The effects of the single, dual, and triple inhibitors were evaluated using proliferation assays and western blotting.

2.9. Statistical analysis

Statistical analyses were performed using Prism software (version 8.0.1; GraphPad Software, La Jolla, CA, USA). Data are presented as mean ± standard error of the mean (SEM). Student's *t*-test was used for the DCFDA ROS assay, and Annexin V/PI staining was analyzed using FACS and western blotting. For combinatorial inhibitor experiments, one-way analysis of variance (ANOVA), followed by Tukey's honestly significant difference test, was used. Proliferation calculations were performed using one-way ANOVA, followed by Dunnett's test. Significant differences were set at $P < 0.05$ and indicated by an asterisk (*). All experiments were replicated at least three times, as indicated in the figure legends.

3. Results

3.1. BBP inhibits GC-1 spg cell proliferation

BBP, which is structured with a benzene ring and a benzyloxycarbonyl moiety (Fig. 1A), was assessed for toxicity in GC-1 spg cells. Various concentrations of BBP were applied for 48 h to determine the IC_{50}. Concentration-dependent toxicity was evident, with a reduced number of GC-1 spg cells observed as BBP concentration increased (Fig. 1B), with marked differences observed in the 12.5 μM BBP treatment, closely aligning with the IC_{20} (12.2 μM) and IC_{50} (53.9 μM) values

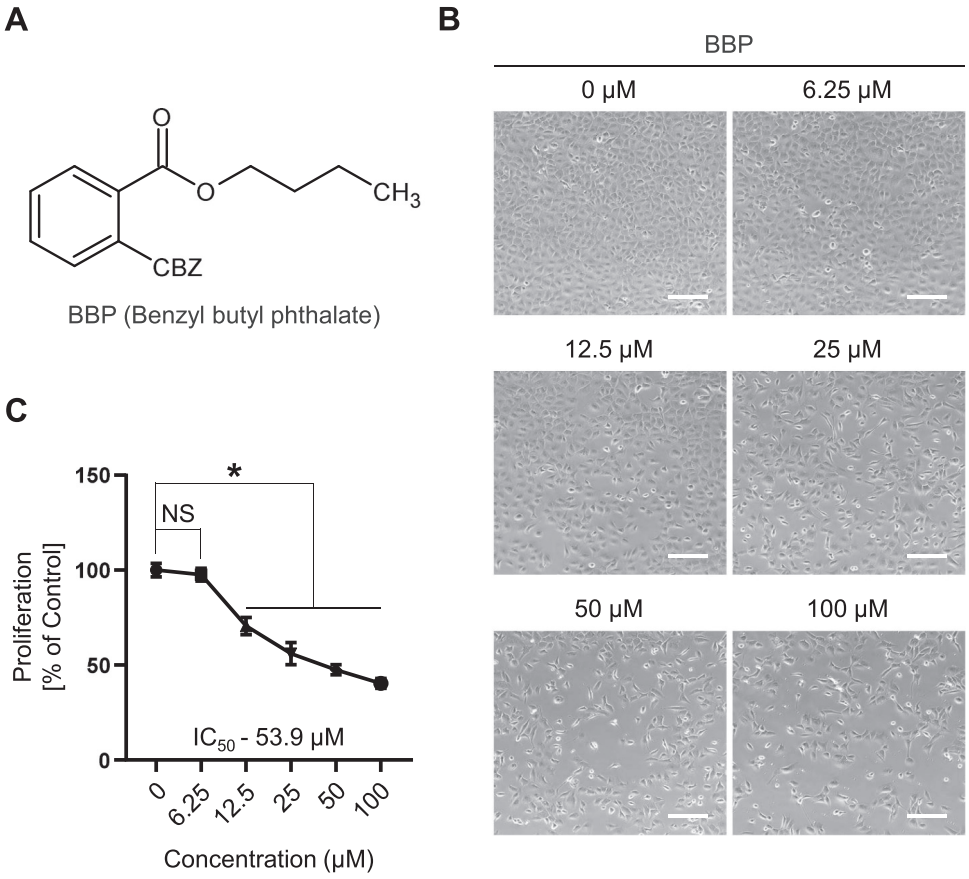

Fig. 1. Benzyl butyl phthalate (BBP) inhibits GC-1 spermatogonia (spg) cell proliferation. **A.** Chemical structure of benzyl butyl phthalate (BBP). **B.** Representative microscopic images of GC-1 spg cells treated with indicated concentrations of BBP for 48 h (Scale bar = 200 μm). **C.** The proliferation rate of GC-1 spg cells is presented as indicated. Values are shown as mean ± SEM. Statistical analysis was performed using one-way ANOVA and multiple comparisons using Dunnett's test, and significant differences between the groups are marked with an asterisk (*$P < 0.05$, n = 5).

of BBP (Fig. 1C). To approximate the IC_{50} value, a concentration of 50 μM BBP was further utilized to assess BBP-induced male germ cell toxicity in this study.

3.2. BBP induces ROS generation and apoptosis

The effects of BBP on ROS generation and the induction of apoptosis were also evaluated. BBP-induced ROS generation was quantitatively determined as the percentage of DCF-positive cells using DCFDA fluorescence microscopy (Fig. 2A). The percentage of DCF-positive GC-1 spg cells increased substantially to 18.5% following treatment with 50 μM BBP compared to the DMSO control (0.9%, Fig. 2B). Furthermore, flow cytometry following annexin V and PI staining demonstrated a substantial increase in apoptotic germ cells treated with 50 μM BBP (Fig. 2C–D), collectively indicating that BBP induces excessive cellular ROS production and apoptosis in GC-1 spg cells.

3.3. BBP triggers both intrinsic and extrinsic apoptosis pathways

Key apoptosis regulator proteins were further evaluated using western blot analysis. BBP at 50 μM substantially increased the expression of intrinsic apoptosis regulator proteins, such as Bcl-2-associated X protein (BAX), cytochrome c, and cleaved-caspase 9 (Fig. 3A–B). Interestingly, BBP induced the expression of the anti-apoptotic protein B-cell lymphoma 2 (BCL2) (Fig. 3A–B). At this concentration, BBP upregulated extrinsic apoptosis regulators, such as FAS and cleaved-caspase 8, leading to the downstream cleavage of caspase 3, caspase 7, and poly (ADP-ribose) polymerase (PARP) compared to the control (Fig. 3A–B), suggesting that BBP-induced proliferation inhibition involves the activation of both intrinsic and extrinsic apoptotic pathways.

3.4. BBP activates autophagy in GC-1 spg cells

Previous studies have indicated phthalate-induced autophagy in male germ cells (Gan et al., 2020; Zhang et al., 2016). Similarly, GC-1 spg cells treated with BBP exhibited substantially more autophagic vesicles (Fig. 4A) and a pronounced increase in the R/GFIR compared with the control (Fig. 4B). We further examined BBP-induced autophagy in GC-1 spg cells by assessing the following marker proteins: autophagy initiator protein (Beclin), autophagosome formation proteins autophagy-related 5 (ATG5) and 7 (ATG7), and selective autophagy receptor protein p62. While Beclin levels showed a slight, non-significant increase, substantial upregulation of ATG and ATG7 expression was observed following BBP treatment (Fig. 4C–D). Phosphor-p62 expression was notably decreased, indicating the activation of autophagy.

3.5. BBP disrupts the phosphorylation levels of key kinase signaling

The PI3K-AKT-mTOR pathway plays a pivotal role in various cellular processes, including survival, proliferation, growth, metabolism, angiogenesis, and metastasis regulation (Ersahin et al., 2015). Marked suppression of phosphorylation of PI3K, AKT, and mTOR was observed following 50 μM BBP treatment compared to the control (Fig. 5A–B). Alterations in PCNA and MAPKs [extracellular signal-regulated kinase (ERK), c-Jun N-terminal kinase (JNK), and p38 MAPK] protein expression levels were examined to elucidate BBP-induced proliferation inhibition in GC-1 cells (Fig. 5C). Whereas PCNA protein expression remained unchanged, the ratios of phosphor-ERK/ERK and phosphor-p38/p38 MAPK substantially increased in the BBP-treated group. Conversely, the phosphor-JNK/JNK ratio decreased markedly (Fig. 5D), indicating that BBP modulated these key kinases, contributing to complex cellular stress and triggering cell death.

3.6. Triple combinatorial treatment mitigates BBP-induced toxicity

To alleviate BBP toxicity, we explored the effects of single, dual, and triple combinatorial treatment using specific inhibitors: PTL (NF-κB), NAC (ROS), and 3-MA (autophagy). We observed no marked recovery in cell proliferation with either the PTL or 3-MA alone treatment (Fig. 6A–6B and Fig. S2A–S2B). Moreover, dual treatment (PTL + NAC and NAC + 3-MA) led to comparable proliferation recovery following BBP exposure; however, the difference was not significant (Fig. 6C–6D and Fig. S2C–S2D). However, the PTL + 3-MA treatment group showed decreased proliferation compared to the BBP exposure group (Fig. 6E and Fig. S2E). A substantial restoration of proliferation was observed under two experimental conditions: NAC as a single treatment and the triple combination treatment of PTL + NAC + 3-MA (Fig. 6F–I). Although the triple combination treatment showed a slightly better recovery than the single NAC treatment, the difference between the two conditions was not statistically significant (data not shown), indicating that NAC-driven proliferation recovery is pivotal in BBP-induced male germ cell toxicity.

The effects of the triple-inhibitor combination were further verified by assessing the expression of apoptosis, autophagy, and proliferation regulatory proteins (Fig. 7A–C). In GC-1 spg cells exposed to 50 μM BBP with the triple inhibitors, cleaved PARP and cytochrome c expression decreased substantially (Fig. 7D–E), whereas phosphor-mTOR expression was restored (Fig. 7F). Additionally, ATG5 and ATG7 expression levels were markedly decreased (Fig. 7G–H).

4. Discussion

BBP is a transitional phthalate derived from alcohols with a straight-chain carbon backbone of C4–C6 (Sedha et al., 2021). Although human studies are limited, BBP has been shown to disrupt vimentin filaments within Sertoli cells and induce apoptosis in spermatogenic cells (Alam and Kurohmaru, 2016). To directly assess the adverse effects of BBP on male germ cells, we examined cell proliferation rates, determining an IC_{50} of 53.9 μM in GC-1 spg cells. Given that multiple crucial signaling pathways intricately regulate male germ cell growth and division, we further investigated BBP's potential to target these pathways and inhibit GC-1 proliferation, uncovering novel findings in this study.

Firstly, BBP induced ROS generation in GC-1 spg cells. Although ROS are natural byproducts of mitochondrial respiration necessary for infection clearance (Dryden, 2018; Reczek and Chandel, 2015), excessive cellular ROS can induce oxidative stress, potentially leading to autophagy and apoptosis (Gan et al., 2020; Li et al., 2019). BBP promotes excessive ROS accumulation in GC-1 spg cells similar to other PAEs in male germ cells (Gan et al., 2020; Li et al., 2019; XueXia et al., 2023; Zhao et al., 2022). Collectively, these and our findings indicate that male germ cells are highly sensitive to oxidative stress.

Secondly, BBP triggered apoptosis in GC-1 spg cells. The apoptotic activity of GC-1 spg cells was markedly increased following BBP exposure. Several other PAEs similarly induce apoptosis (Chen et al., 2022; Gan et al., 2020; Li et al., 2019; XueXia et al., 2023; Zhao et al., 2022), as shown in the current study. BBP exposure induced a marked increase in BAX, cytochrome c, and cleaved caspase-9 levels, indicating the activation of mitochondrial apoptosis. No significant changes were observed in the BAX/BCL2 ratio. Increased BCL2 protein levels suggested the activation of a complex survival response to counteract BBP-induced BAX activity. Extrinsic pathways (Kiraz et al., 2016; Kischkel et al., 1995; Slee et al., 2001) are also activated by BBP, as evidenced by the marked increase in FAS and cleaved caspase-8, and cleaved caspase-3, −7, and PARP protein levels. These results indicate that BBP induces potent intrinsic (mitochondria-mediated) and extrinsic (membrane receptor-mediated) male germ cell apoptosis.

Thirdly, BBP-induced toxicity in GC-1 spg cells is associated with autophagy activation, a crucial protective mechanism (Filomeni et al., 2015) that prevents cellular damage during nutrient shortages or

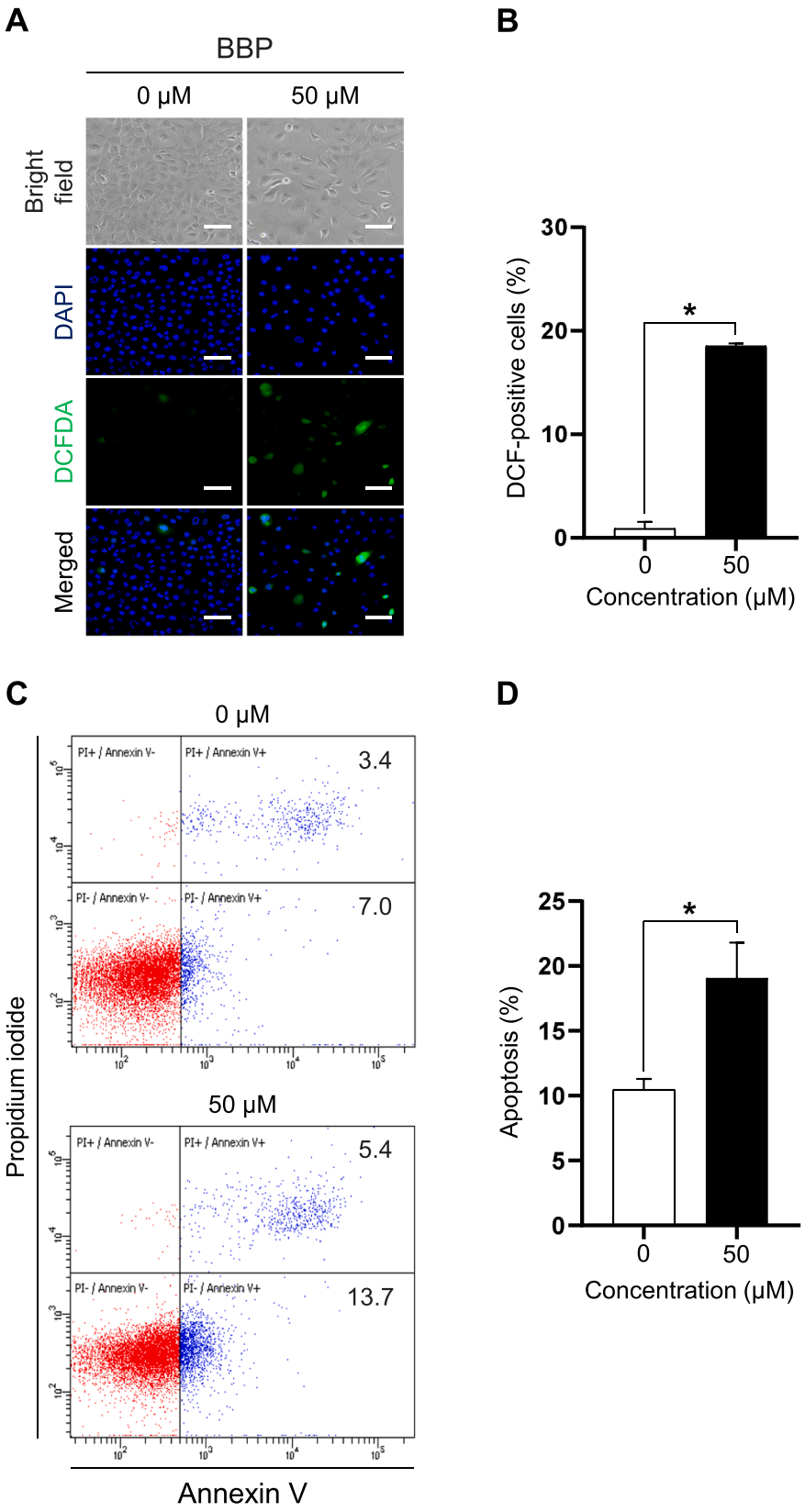

Fig. 2. Benzyl butyl phthalate (BBP) induces reactive oxygen species (ROS) generation and triggers apoptosis. **A**. Representative microscopic images of GC-1 spermatogonia (spg) cells treated with 0 μM and 50 μM BBP for 48 h. Fluorescent microscopic images of oxidized dichlorofluorescein (DCF) by ROS are presented (4′,6-diamidino-2-phenylindole [DAPI] for nucleus staining, scale bar = 100 μm). **B**. A graphical representation of **A**, showing dichlorofluorescein diacetate (DCFDA)-positive GC-1 spg cells as a percentage (n = 3). **C**. Representative fluorescence-activated cell sorting (FACS) images of early and late apoptotic cells as a percentage. **D**. A graphical representation of **C** is shown (n = 3). Values are expressed as the mean ± SEM. Statistical analysis was performed using Student's *t*-tests, and significant differences between the groups are indicated with an asterisk (*$P < 0.05$).

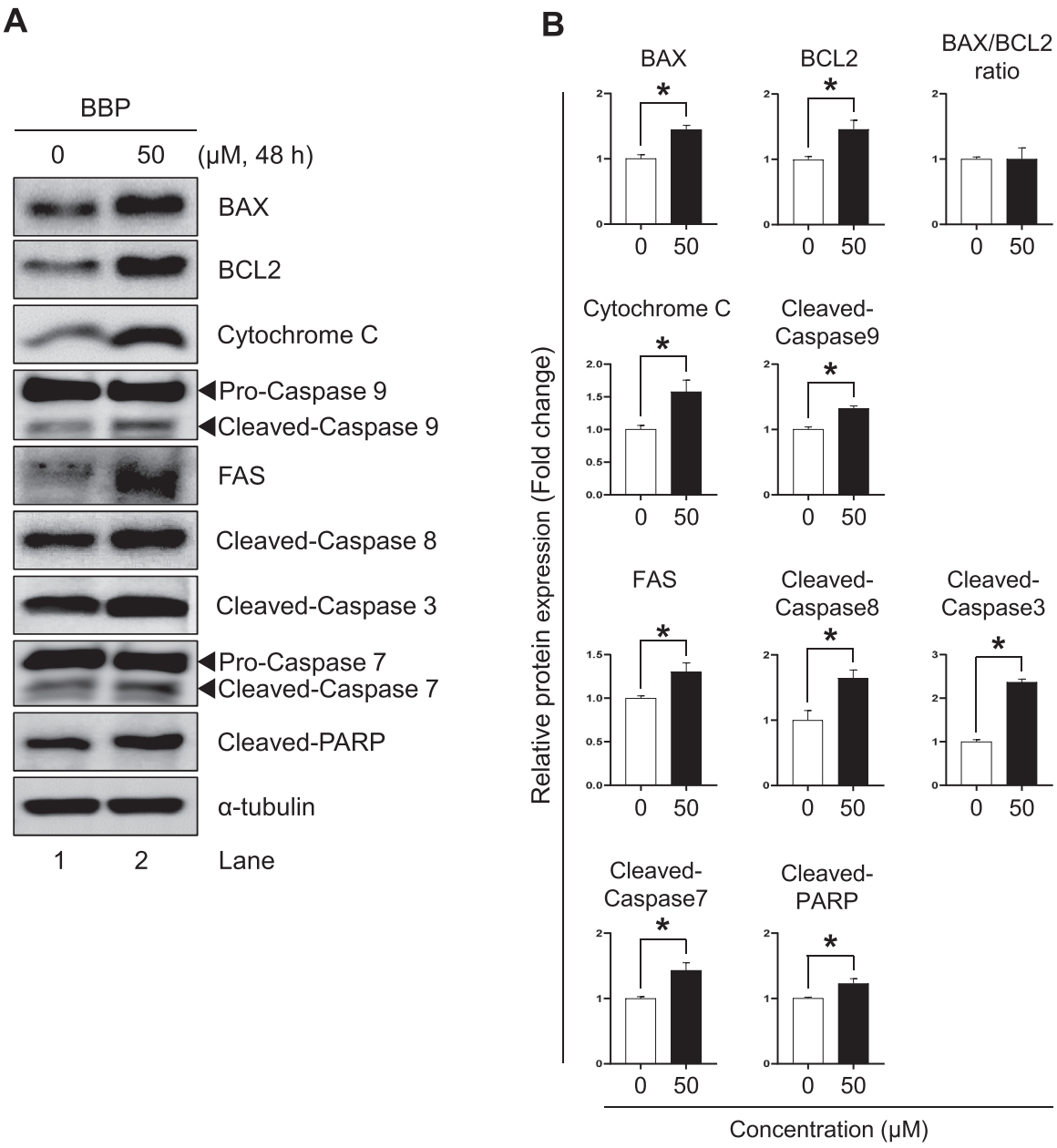

Fig. 3. Benzyl butyl phthalate (BBP) activates both intrinsic and extrinsic apoptosis.
A. Representative western blot images of key apoptosis mediators for intrinsic (BAX, BCL2, cytochrome c, and cleaved-caspase 9), extrinsic (FAS, cleaved-caspase 8), and executioner proteins (cleaved-caspase 3, cleaved-caspase 7, PARP). **B.** Graphical presentations of protein expressions are shown in **A**. All data are displayed as the mean ± SEM. Statistical analysis was performed using Student's *t*-test, and statistically significant differences are indicated with an asterisk. (*$P < 0.05$, n = 3). Abbreviations: BCL2, B-cell lymphoma 2; BAX, Bcl-2-associated X protein; PARP, Poly (ADP-ribose) polymerase.

defends against cytotoxic stimuli (Noguchi et al., 2020). Substantial acridine orange staining represented late-stage autophagy activation by BBP, as indicated by augmented autophagic vesicles. Moreover, the levels of autophagy proteins, Beclin, ATG5, and ATG7, substantially increase and those of phosphor-p62 decrease (Changotra et al., 2022; Djavaheri-Mergny et al., 2010; Eisenberg-Lerner et al., 2009; Ichimura and Komatsu, 2010; Parzych and Klionsky, 2014).

Fourthly, the pivotal cell proliferation regulator proteins, PI3K, AKT, mTOR (Deng et al., 2021), PCNA, and MAPK kinases have been investigated for their significance in cell proliferation, division, and differentiation (Cuadrado and Nebreda, 2010; Juríková et al., 2016; Sun et al., 2015; Weston and Davis, 2002). Whereas PCNA protein expression level remained unchanged, the phosphorylation levels of other proteins were substantially altered by BBP. Furthermore, *Ccne* and *Cdk2* levels were markedly decreased by BBP (data not shown), indicating that BBP inhibits germ cell vitality through complex mechanisms affecting multiple pathways.

Lastly, the inhibitors selected for BBP toxicity were PTL, NAC, and 3-MA, which are known for their activities to counteract apoptosis, oxidative stress, and autophagy induced by toxicants and hydrogen peroxide-induced ROS (Gan et al., 2020; Liu et al., 2020; Mao and Zhu, 2018). Although PTL and 3-MA alone showed no recovery effects, NAC markedly alleviated the effects of BBP. Dual treatments such as PTL + NAC and NAC + 3-MA showed slightly increased but non-significant protective effects, whereas PTL + 3-MA treatment did not affect cell proliferation. Compared to the single and dual treatments, triple treatment with PTL, NAC, and 3-MA demonstrated effective synergistic effects, with NAC making a major contribution to the effect of combined

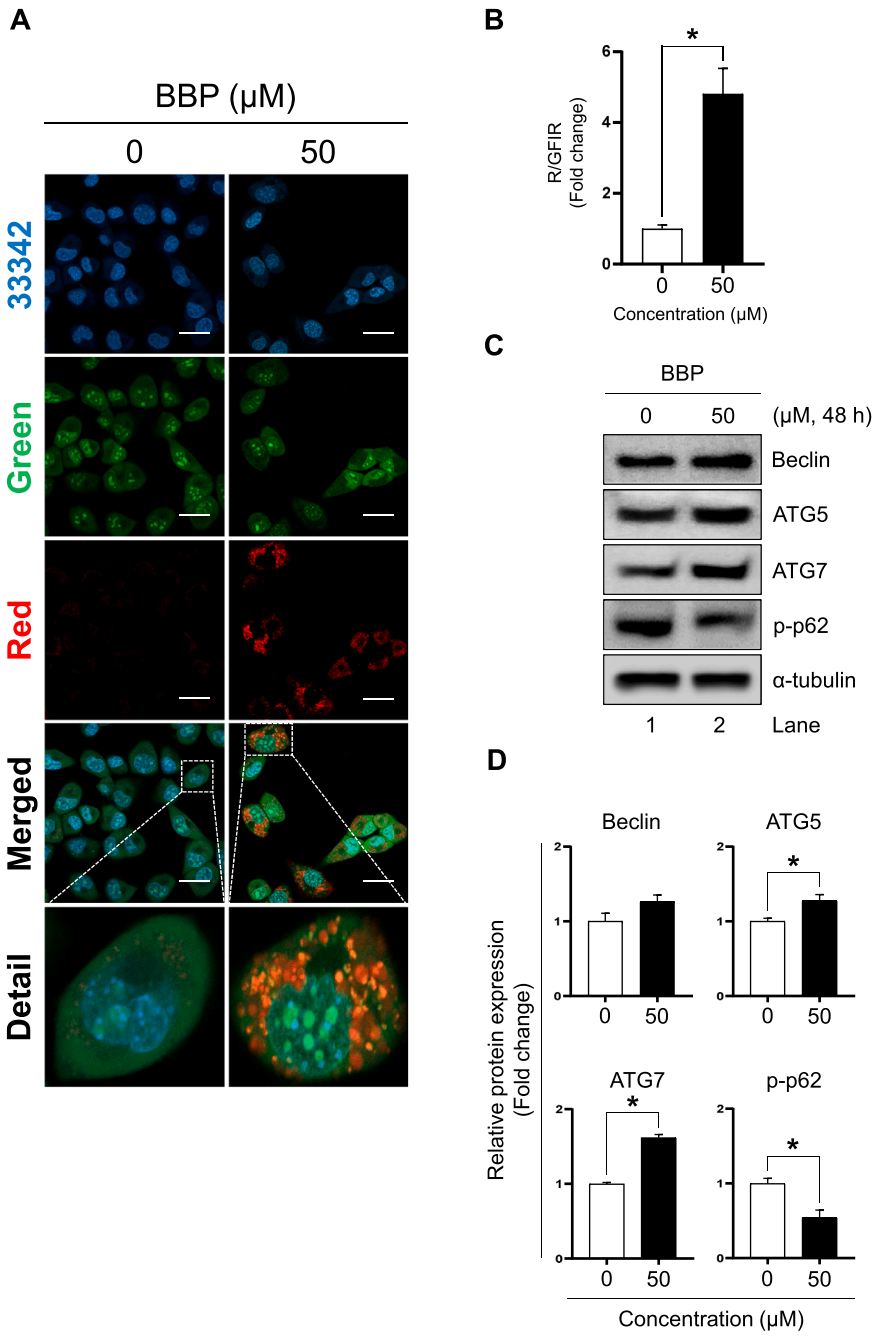

Fig. 4. Benzyl butyl phthalate (BBP) induces autophagy activation. **A.** Representative confocal microscopic images of AO-stained GC-1 spermatogonia cells depicting autophagy induction and vesicle formation between the control and BBP-treated groups (Scale bar = 50 μm). **B.** Graphical representation of red-to-green fluorescence intensity ratio (R/GFIR). **C.** Representative images of autophagy regulator protein expressions (Beclin for initiator of autophagy; autophagy-related 5 [ATG5] and autophagy-related 7 [ATG7] for autophagosome formation; p62 for cargo recognition and autophagosome maturation). **D.** Graphical representation of protein expressions shown in **C.** Values are normalized to α-tubulin and presented as the mean ± SEM. Statistical analysis was performed using Student's *t*-tests and statistically significant differences are indicated with an asterisk ($^*P < 0.05$, n = 3).

alleviation. The protein levels of cytochrome c, cleaved PARP, ATG5, ATG7, and mTOR were restored by the triple inhibitor treatment. Given the alleviating effect of NAC, the hypothesis that BBP can trigger oxiapoptophagy resulting from excessive oxidative stress, leading to both apoptosis and autophagy (Nury et al., 2021), needs further investigation.

Our findings in the current study demonstrate that BBP induces cellular ROS generation, apoptosis, and autophagy, and suppresses PI3K, AKT, mTOR, and JNK, while increasing ERK and p38 MAPK phosphorylation, leading to cell death in GC-1 spg cells. Importantly, the triple combination treatment of PTL, NAC, and 3-MA, mitigated BBP-induced cellular stress. These results offer novel insights into BBP-induced male germ cell toxicity as a potential infertility factor and suggest potential therapeutic interventions.

5. Conclusion

This study provides new insights into the impact of BBP on male germ cells and explores potential therapeutic interventions. BBP inhibits GC-1 spg cell proliferation by inducing ROS and cell death while altering vital PI3K-AKT-mTOR and MAPK signaling. The triple combination treatment (PTL, NAC, and 3-MA) alleviated BBP toxicity and restored

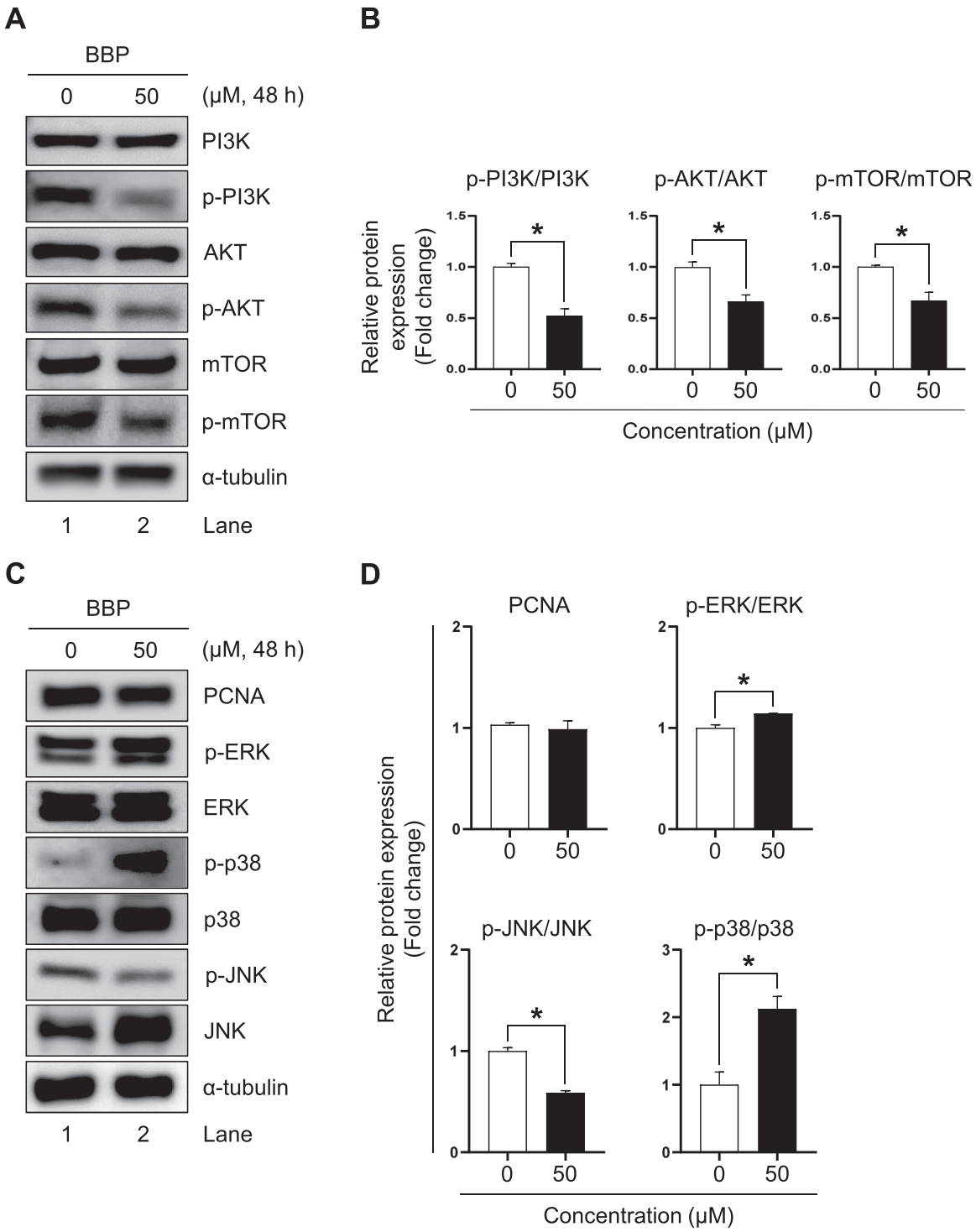

Fig. 5. Benzyl butyl phthalate (BBP) inhibits phosphorylation of key signaling proteins **A**. Representative western blot images of phosphoinositide 3-kinase (PI3K), AKT serine/Threonine kinase 1, and mammalian target of rapamycin (mTOR) protein expressions in GC-1 spermatogonia (spg) cells treated with BBP for 48 h. **B**. Relative protein expressions shown in **A** are presented in graphs. **C**. Representative western blot images showing proliferating cell nuclear antigen (PCNA), extracellular signal-regulated kinase (ERK) c-Jun N-terminal kinases (JNK), and p38 MAPK protein expressions in GC-1 spg cells exposed to BBP for 48 h; including PCNA, phosphor-ERK (p-ERK), total ERK, phosphor-JNK, total JNK, and phosphor-p38 MAPK, and total p38 MAPK. **D**. Graphical representation of western blot data shown in **C**. All values are exhibited as the mean ± SEM. Statistical analysis was determined using Student's *t*-tests and statistically significant differences are presented with an asterisk (*$P < 0.05$, n = 3).

cell proliferation, potentially by suppressing apoptosis and autophagy. These findings demonstrate the toxicity of BBP in male germ cells and suggest its potential therapeutic implications for environmental toxin management.

Funding

This study was supported by the Basic Science Research Program of the National Research Foundation of Korea (NRF), funded by the Ministry of Education (NRF-2018R01A6A1A03025159) and the Korea

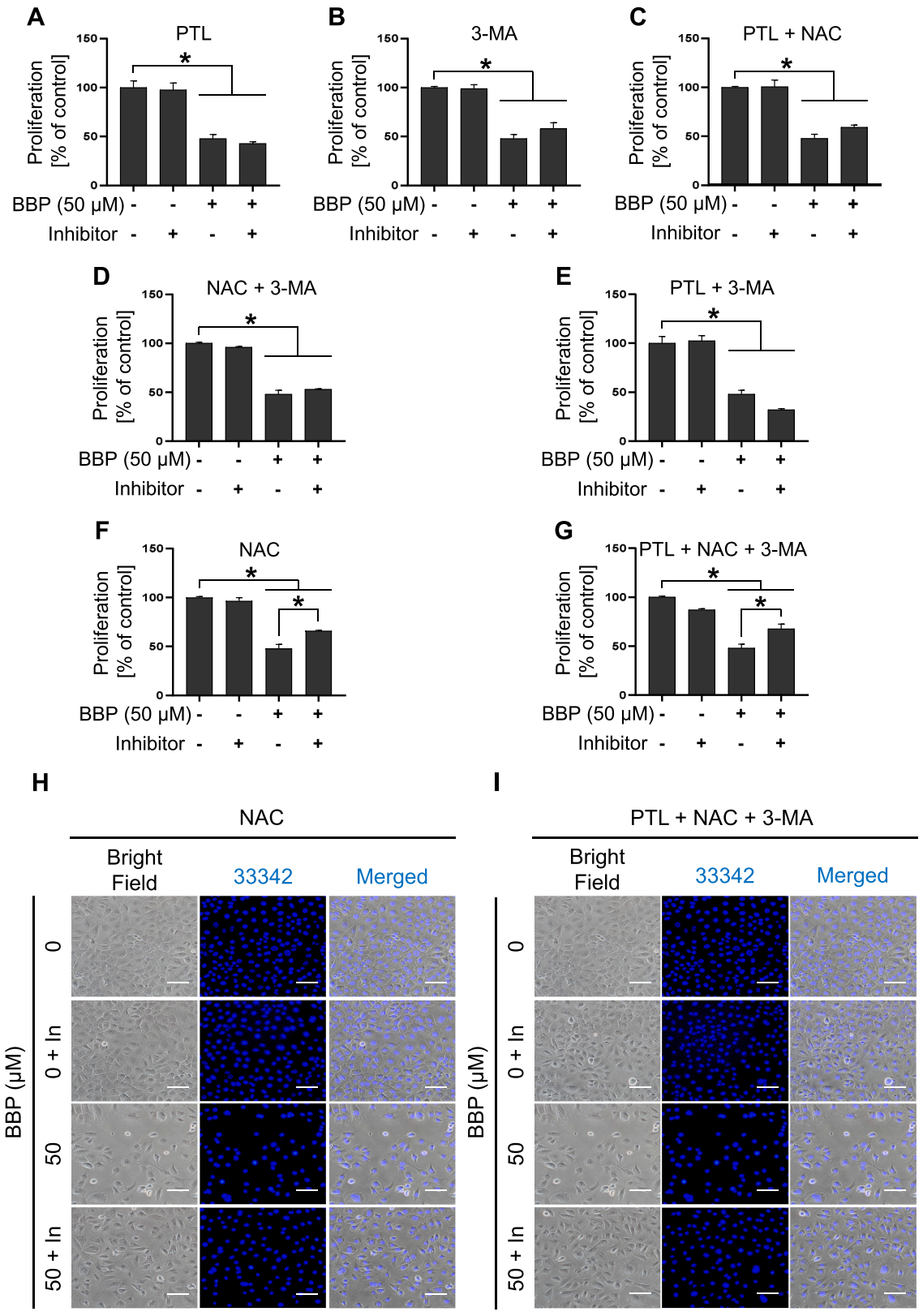

Fig. 6. Efficacy of parthenolide (PTL), N-acetylcysteine (NAC), and 3-methyladenine (3-MA) in counteracting benzyl butyl phthalate (BBP) toxicity. **A–B**. Graphical representation of the proliferation rates and alleviating effects of individual inhibitors in single treatments. **C–E**. Results of dual combination treatments. **F**. Outcomes of NAC treatment **G**. Results of the triple combination treatment. **H**. Representative microscopic images showing proliferation rates after NAC treatment (**F**). **I**. Representative microscopic images illustrating the proliferation rates after the triple combination treatment (**G**). All proliferation data are indicated as the mean ± SEM. Statistical analyses were performed using one-way analysis of variance and multiple comparisons using Tukey's honest significant difference test (*$P < 0.05$, n = 3). Abbreviations: In, inhibitors.

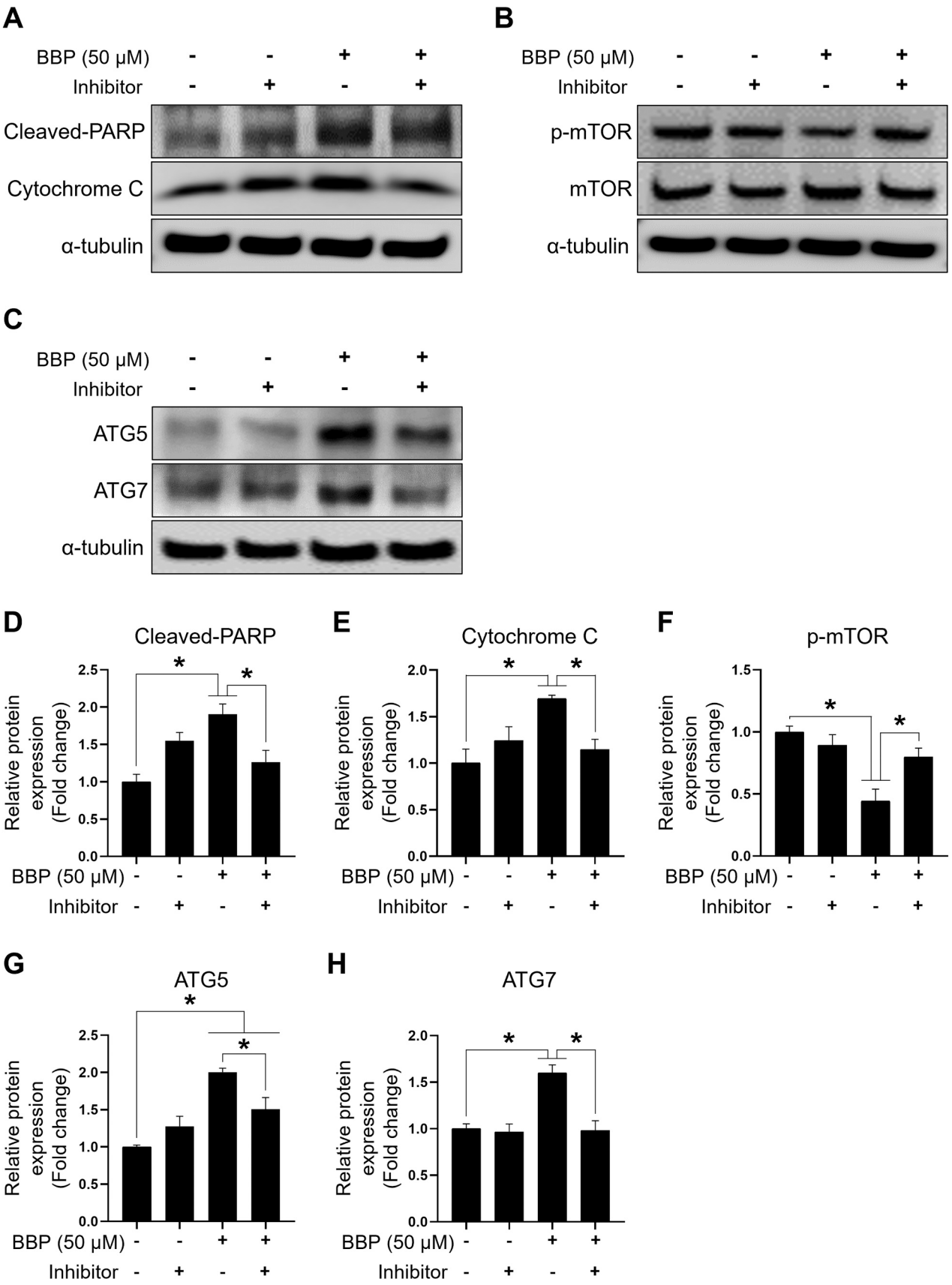

Fig. 7. Triple combination treatment mitigates apoptosis and autophagy and restores mTOR phosphorylation. **A–C.** Representative western blot images of poly (ADP-ribose) polymerase (PARP), cytochrome c, phosphorylated mammalian target of rapamycin (p-mTOR), and autophagy-related 5 (ATG5) and 7 (ATG7) expression. **D–H.** Graphical representation of protein expression shown in **A–C.** Each protein expression was normalized to α-tubulin and is exhibited as the mean ± SEM. Statistical analyses were conducted using one-way analysis of variance and multiple comparisons using Tukey's honest significant difference test (*$P < 0.05$, n = 3).

Institute of Marine Science and Technology Promotion (KIMST), funded by the Ministry of Oceans and Fisheries, Korea (RS-2023–00235057).

CRediT authorship contribution statement

Seok-Man Kim: Conceptualization, data curation, methodology, formal analysis, and writing of the original draft. **Gil Un Han:** Investigation and validation. **Seul Gi Kim:** Investigation and validation. **Sung-Hwan Moon:** Resources, writing, review, and editing. **Seung Hee Shin:** Methodology, formal analysis, writing, review, and editing. **Buom-Yong Ryu:** Conceptualization, validation, supervision, review, and editing.

Declaration of Competing Interest

The authors declare that they have no known competing financial interests or personal relationships that could have appeared to influence the work reported in this paper.

Data availability

Data will be made available on request.

Acknowledgments

We thank J. Kim for the technical assistance at the BT Research Facility Center, Chung-Ang University.

Appendix A. Supporting information

Supplementary data associated with this article can be found in the online version at doi:10.1016/j.ecoenv.2024.116544.

References

Ahmad, R., et al., 2014. Effects of in utero di-butyl phthalate and butyl benzyl phthalate exposure on offspring development and male reproduction of rat. Environ. Sci. Pollut. Res Int 21, 3156–3165.
Alam, M.S., Kurohmaru, M., 2016. Butylbenzyl phthalate induces spermatogenic cell apoptosis in prepubertal rats. Tissue Cell 48, 35–42.
Aso, S., et al., 2005. A two-generation reproductive toxicity study of butyl benzyl phthalate in rats. J. Toxicol. Sci. 30, S39–S58.
Changotra, H., et al., 2022. ATG5: A central autophagy regulator implicated in various human diseases. Cell Biochem Funct. 40, 650–667.
Chen, J., et al., 2022. Di-isononyl phthalate induces apoptosis and autophagy of mouse ovarian granulosa cells via oxidative stress. Ecotoxicol. Environ. Saf. 242, 113898.
Cuadrado, A., Nebreda, A.R., 2010. Mechanisms and functions of p38 MAPK signalling. Biochem. J. 429, 403–417.
da Silva Costa, R., et al., 2021. Potential risk of BPA and phthalates in commercial water bottles: A minireview. J. Water Health 19, 411–435.
Darbre, P.D., 2022. What are endocrine disrupters and where are they found? Endocrine Disruption and Human Health. Elsevier, pp. 3–29.
Deng, C.-Y., et al., 2021. The role of the PI3K/AKT/mTOR signalling pathway in male reproduction. Curr. Mol. Med. 21, 539–548.
Djavaheri-Mergny, M., et al., 2010. Cross talk between apoptosis and autophagy by caspase-mediated cleavage of Beclin 1. Oncogene 29, 1717–1719.
Dominguez, F., 2019. Phthalates and other endocrine-disrupting chemicals: the 21st century's plague for reproductive health. Fertil. Steril. 111, 885–886.
Dryden, M., 2018. Reactive oxygen species: a novel antimicrobial. Int J. Antimicrob. Agents 51, 299–303.
Eisenberg-Lerner, A., et al., 2009. Life and death partners: apoptosis, autophagy and the cross-talk between them. Cell Death Differ. 16, 966–975.
Ersahin, T., et al., 2015. The PI3K/AKT/mTOR interactive pathway. Mol. Biosyst. 11, 1946–1954.
Fayomi, A.P., Orwig, K.E., 2018. Spermatogonial stem cells and spermatogenesis in mice, monkeys and men. Stem Cell Res. 29, 207–214.
Filomeni, G., et al., 2015. Oxidative stress and autophagy: the clash between damage and metabolic needs. Cell Death Differ. 22, 377–388.
Gan, Y., et al., 2020. Di-2-ethylhexyl phthalate (DEHP) induces apoptosis and autophagy of mouse GC-1 spg cells. Environ. Toxicol. 35, 292–299.
Gao, D.-W., Wen, Z.-D., 2016. Phthalate esters in the environment: a critical review of their occurrence, biodegradation, and removal during wastewater treatment processes. Sci. Total Environ. 541, 986–1001.
Gledhill, W.E., et al., 1980. An environmental safety assessment of butyl benzyl phthalate. Environ. Sci. Technol. 14, 301–305.
Hofmann, M.C., et al., 1992. Immortalization of germ cells and somatic testicular cells using the SV40 large T antigen. Exp. Cell Res 201, 417–435.
Ichimura, Y., Komatsu, M., 2010. Selective degradation of p62 by autophagy. Semin Immunopathol. 32, 431–436.
Juríková, M., et al., 2016. Ki67, PCNA, and MCM proteins: Markers of proliferation in the diagnosis of breast cancer. Acta Histochem. 118, 544–552.
Kavlock, R., et al., 2002. NTP Center for the Evaluation of Risks to Human Reproduction: phthalates expert panel report on the reproductive and developmental toxicity of butyl benzyl phthalate. Reprod. Toxicol. (5), 453–487.
Kiraz, Y., et al., 2016. Major apoptotic mechanisms and genes involved in apoptosis. Tumour Biol. 37, 8471–8486.
Kischkel, F.C., et al., 1995. Cytotoxicity-dependent APO-1 (Fas/CD95)-associated proteins form a death-inducing signaling complex (DISC) with the receptor. EMBO J. 14, 5579–5588.
Kubota, H., Brinster, R.L., 2018. Spermatogonial stem cells. Biol. Reprod. 99, 52–74.
Li, R., et al., 2019. Di-n-butyl phthalate epigenetically induces reproductive toxicity via the PTEN/AKT pathway. Cell Death Dis. 10, 307.
Liu, T., et al., 2020. Effects of nonylphenol induced oxidative stress on apoptosis and autophagy in rat ovarian granulosa cells. Chemosphere 261, 127693.
Lv, Y., et al., 2019. Benzyl butyl phthalate non-linearly affects rat Leydig cell development during puberty. Toxicol. Lett. 314, 53–62.
Mao, W., Zhu, Z., 2018. Parthenolide inhibits hydrogen peroxide-induced osteoblast apoptosis. Mol. Med Rep. 17, 8369–8376.
Nagao, T., et al., 2000. Effect of butyl benzyl phthalate in Sprague-Dawley rats after gavage administration: a two-generation reproductive study. Reprod. Toxicol. 14, 513–532.
Net, S., et al., 2015. Occurrence, fate, behavior and ecotoxicological state of phthalates in different environmental matrices. Environ. Sci. Technol. 49, 4019–4035.
Noguchi, M., et al., 2020. Autophagy as a modulator of cell death machinery. Cell Death Dis. 11, 517.
Nury, T., et al., 2021. Oxiapoptophagy: A type of cell death induced by some oxysterols. Br. J. Pharmacol. 178, 3115–3123.
Parzych, K.R., Klionsky, D.J., 2014. An overview of autophagy: morphology, mechanism, and regulation. Antioxid. Redox Signal 20, 460–473.
Reczek, C.R., Chandel, N.S., 2015. ROS-dependent signal transduction. Curr. Opin. Cell Biol. 33, 8–13.
Sedha, S., et al., 2021. Reproductive toxic potential of phthalate compounds - State of art review. Pharm. Res 167, 105536.
Sharma, A., et al., 2020. Endocrine-disrupting chemicals and male reproductive health. Reprod. Med Biol. 19, 243–253.
Shin, E.M., et al., 2014. DEAD-box helicase DP103 defines metastatic potential of human breast cancers. J. Clin. Invest 124, 3807–3824.
Slee, E.A., et al., 2001. Executioner caspase-3, -6, and -7 perform distinct, non-redundant roles during the demolition phase of apoptosis. J. Biol. Chem. 276, 7320–7326.
Staples, C.A., et al., 1997. The environmental fate of phthalate esters: a literature review. Chemosphere 35, 667–749.
Sun, Y., et al., 2015. Signaling pathway of MAPK/ERK in cell proliferation, differentiation, migration, senescence and apoptosis. J. Recept. Signal Transduct. 35, 600–604.
Toma, C.C., et al., 2017. New extraction technologies for Syringa vulgaris (Oleaceae) meristematic extracts. Rev. De. Chim. (Buchar.) 68, 1796–1798.
Weston, C.R., Davis, R.J., 2002. The JNK signal transduction pathway. Curr. Opin. Genet. Dev. 12, 14–21.
XueXia, L., et al., 2023. Di-2-ethylhexyl phthalate (DEHP) exposure induces sperm quality and functional defects in mice. Chemosphere 312, 137216.
Yu, D., et al., 2021. Improved detection of reactive oxygen species by DCFH-DA: New insight into self-amplification of fluorescence signal by light irradiation. Sens. Actuators B: Chem. 339.
Zhang, G., et al., 2016. DBP-induced endoplasmic reticulum stress in male germ cells causes autophagy, which has a cytoprotective role against apoptosis in vitro and in vivo. Toxicol. Lett. 245, 86–98.
Zhao, Y., et al., 2022. Phthalate-induced testosterone/androgen receptor pathway disorder on spermatogenesis and antagonism of lycopene. J. Hazard Mater. 439, 129689.